ACS APPLIED MATERIALS & INTERFACES

Research Article

www.acsami.org

In Situ Formed Ionic Liquids in Synthetic Esters for Significantly Improved Lubrication

Mingjin Fan, Zenghong Song, Yongmin Liang, Feng Zhou,* and Weimin Liu*

State Key Laboratory of Solid Lubrication, Lanzhou Institute of Chemical Physics, Chinese Academy of Sciences, Lanzhou 730000, China.

ABSTRACT: A novel way of in situ forming ionic liquids (ILs) in synthetic esters is presented. Lithium bis(trifluoromethylsulfonyl)imide (LiTFSI) can form ILs with synthetic esters, [Li(synthetic ester)]TFSI, by the donation of lone pairs on carbonyl oxygen atoms of an ester molecule to a lithium ion to form a weakly Lewis-acidic complex cation [Li(synthetic ester)]$^+$ and following interaction with the weakly Lewis-basic anion TFSI$^-$ to generate [Li(synthetic ester)]TFSI. LiTFSI has high solubility in synthetic esters because of the complex formation. The physicochemical and tribological properties of [Li(synthetic ester)]TFSI as lubricant additives were investigated. The easy preparation, extremely good solubility and excellent tribological properties of the type of ILs make them great advantages as compared with conventional ILs that can hardly be used as lubricant additives in synthetic esters due to their low solubility. The lubrication mechanism of these ILs is tentatively discussed.

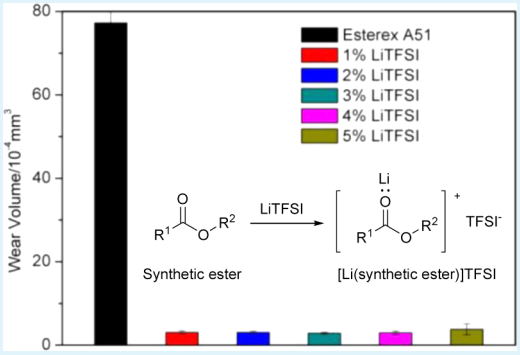

KEYWORDS: *lithium bis(trifluoromethylsulfonyl)imide, coordination, ionic liquid, synthetic ester, lubricant additive*

INTRODUCTION

As a key addition to their widespread applications ranging from organic synthesis and catalysis, separation science to electrochemistry,[1−6] ionic liquids (ILs) have been long established as a novel versatile lubricant because of their unique properties such as negligible volatility, nonflammability and high-thermal stability.[7−13] Unfortunately, the high cost and tedious procedure for preparing ILs are main problems to put them into industrial application after ten years of extensive development. In addition, their low solubility severely restricts their application as lubricant additives for most base oils.[14] The development of new ILs with improved performance and decreased cost is one of the main goals of our research. We recently reported a new concept of in situ preparation IL lubricant additives in polyethylene glycol (PEG).[15] It provides a new strategy toward industrial application of ILs without the synthesis of ILs. It undoubtedly simplifies procedures of ILs preparation and lowers the cost. In this paper, we extend our study to in situ formation of ILs in synthetic esters by the donation of lone pairs on carbonyl oxygen atoms of an ester molecule to a lithium ion to form a weakly Lewis acidic complex cation [Li(synthetic ester)]$^+$ and following interaction with the weakly Lewis-basic anion TFSI$^-$ to generate [Li(synthetic ester)]TFSI. It is well-known that synthetic esters are commonly used lubricating oils, especially for combustion engines, but conventional ILs have very low solubility in synthetic esters, making them hardly used in these oils. However, the current strategy allows in situ forming ILs and provides a convenient and practical way to get ILs with extremely good solubility in synthetic ester. Considering few studies have been devoted to the interaction between lithium salts and esters without $-(CH_2CH_2O)-$ or $-(CH_2CH_2COO)-$ chain units,[16−18] we report herein the physicochemical evidence of the in situ formed [Li(synthetic ester)]TFSI and their characterization as lubricant additives.

EXPERIMENTAL SECTION

Chemicals. The following reagents and materials were used as received: lithium bis(trifluoromethylsulfonyl)imide (LiTFSI), bis(2-ethylhexyl)adipate (DEHA) and bis(2-ethylhexyl)sebacate (DEHS) (ACROS), and Esterex adipate ester A51 (Exxon Mobil Companies). Pentaerythritol oleate (PETO) and trihydroxymethylpropyl trihexacetate (TMPTH) were synthesized by our laboratory. Imidazolium tetrafluoroborate (L-B102), 1-ethyl-3-methyl imidazolium bis(trifluoromethylsulfonyl)imide (L-F102), 1-butyl-3-methyl imidazolium bis(trifluoromethylsulfonyl)imide (L-F104), and 1-methyl-3-hexylimidazolium hexafluorophosphate (L-P106) were synthesized according to the literature.[19] The lubricants were prepared by stirring a certain amount (1%, 2%, etc.) of LiTFSI in the esters at room temperature (RT) until it was totally dissolved. All the other chemicals used in the synthesis were of AR grade.

Spectroscopic Characterization. The FTIR spectra of the samples were recorded on a Nicolet iS10 FT-IR spectrometer between 4000 and 400 cm^{-1} with a resolution of 2 cm^{-1}. A droplet of the liquid sample was spread on a dry KBr piece for the infrared (IR) spectroscopic measurements.

Thermal Analysis. The phase transition temperatures of the complex systems were measured on a DSC 200F3 differential scanning

Received: September 3, 2012
Accepted: November 27, 2012
Published: November 27, 2012

   dx.doi.org/10.1021/am3018042 | ACS Appl. Mater. Interfaces 2012, 4, 6683−6689

Scheme 1. Proposed in Situ Formation of [Li(synthetic ester)]TFSI and the Chemical Structures of DEHA, DEHS, TMPTH, and PETO

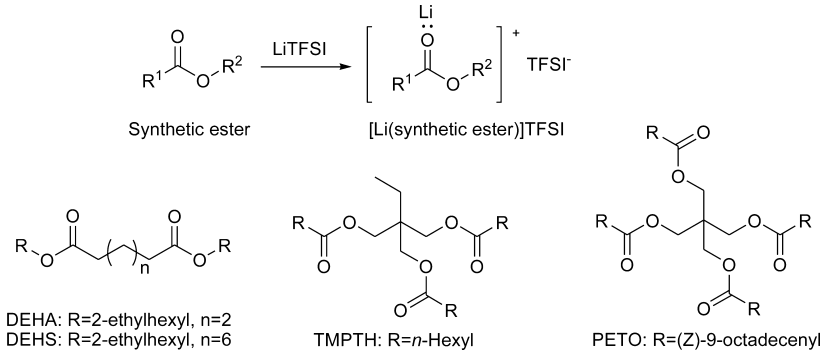

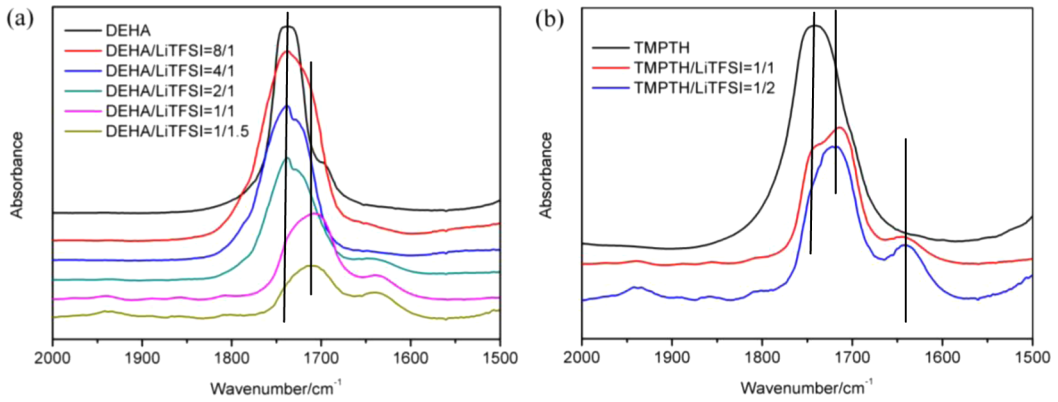

Figure 1. FTIR spectra of the C═O stretching mode of (a) pure DEHA and DEHA−LiTFSI and (b) pure TMPTH and TMPTH−LiTFSI complex systems at various molar ratios.

calorimeter (DSC, NET ZSCH). The sample were first cooled to about −130 °C with liquid nitrogen and then heated to 70 °C at a rate of 10.0 K/min. The thermal behavior of the samples was carried out on an STA 449 C Jupiter simultaneous TG-DSC instrument. The temperature was programmed to increase from the initial temperature of 20 °C to approximately 600 °C, at a rate of 10 °C/min in air. The weight loss and heat flow values were monitored in the TG-DSC analysis.

Viscosity and Copper Strip Test. The kinematic viscosity of the lubricants was carried out on a SYP1003-III viscometer at 40 and 100 °C, respectively. The copper strip test was performed using the GB-T5096−1985 (91) procedure. A piece of bright finish copper was immersed within a certain amount of specimen. This was heated at 100 °C for 3 h. At the end of the test, the copper was taken out and washed for comparison with the corrosion standard tint board.

Friction and Wear Test. The friction and wear tests were carried out on an Optimol SRV-IV oscillating reciprocating friction and wear tester. The contact between the frictional pair was achieved by pressing the upper running ball against the lower stationary disk which was driven to reciprocate at a given frequency and displacement. The upper ball is AISI 52100 steel with 10 mm diameter and approximately 61−64HRC hardness. The lower stationary disk is AISI52100 steel with Φ24 mm ×7.9 mm and hardness of approximately 61−64HRC hardness. The friction and wear tests in this work were conducted at amplitude of 1 mm and frequency of 25 Hz. The relative humidity was 20−50%. The wear volume of the lower disk was measured by a MicroXAM 3D noncontact surface mapping profiler.

The morphology of the worn surfaces was analyzed by a JSM-5600LV scanning electron microscope (SEM). The XPS analysis was carried out on a K-Alpha X-ray photoelectron spectrometer (XPS) using Al Ka radiation as the exciting source. The samples were rinsed three times with ultrasonic in ethanol before scanning. The binding energy of the target elements was determined at a pass energy of 50.0 eV with a resolution of about ±0.3 eV. The binding energy of contaminated carbon (C1s = 284.6 eV) was used as the reference.

RESULTS AND DISCUSSION

Spectroscopic Characterization. The proposed in situ forming [Li(synthetic ester)]TFSI was shown in Scheme 1. The assignments of IR bands are reasonable to confirm the coordination between Li^+ and C═O groups of synthetic esters and will be adopted in this paper.[20] Four types of synthetic esters: DEHA, DEHS, TMPTH, and PETO were used as base oils to prove the generality of this coordination (their chemical structures are shown in Scheme 1). Figure 1a shows the IR spectra between 1500 and 2000 cm^{-1} of DEHA/LiTFSI complex systems at different molar ratios. The strong band at 1737 cm^{-1} in the IR spectrum of pure DEHA is attributed to its C═O stretching. This C═O stretching band changes significantly upon introducing LiTFSI in the system owing to the influences of the Li^+-O coordination. It is a common feature for the formation of a complex between Li^+ and C═O group that the lone pairs on O atoms tend to transfer from O to Li^+ resulting in the weakening of the double bond characteristic of C═O group. So the C═O stretching band is broadened and shifts to lower frequency with increasing LiTFSI content. The position of the C═O stretching band shifts from 1737 to 1708 cm^{-1} for the LiTFSI/DEHA complex system at 1/1 molar ratio and almost no band at 1737 cm^{-1} can be detected probably due to the disappearance of free DEHA molecules in this system. Further increasing LiTFSI content, such as 1/1.5, has no significant influence on the spectrum. Similarly, the position of the C═O stretching band shifts from 1739 to 1705 cm^{-1} for

dx.doi.org/10.1021/am3018042 | ACS Appl. Mater. Interfaces 2012, 4, 6683−6689

the DEHS/LiTFSI complex system at 1/1 molar ratio. Obvious spectral changes are also observed from the spectra of TMPTH−LiTFSI and PETO−LiTFSI complex systems at 1/1 molar ratio. But in these spectra, two C═O stretching bands can be detected due to the existence of free ester molecules in the two complex systems at this molar ratio. The spectra of TMPTH−LiTFSI systems at molar ratio of 1/1 and 1/2 are shown in Figure 1b as an example. The two C═O stretching bands are attributed to the C═O stretching of free TMPTH molecules and coordinated TMPTH molecules, respectively. The position of the C═O stretching band shifts from 1740 to 1722 cm^{-1} for TMPTH-LiTFSI system at 1/2 molar ratio and almost no band at 1740 cm^{-1} can be detected. It indicates that no free TMPTH molecule exits in the system at this molar ratio. These studies clearly indicate that the lithium ions coordinate with the carbonyl oxygen atoms of synthetic esters. It is reasonable to assume that one Li^+ at least tends to coordinate with two carbonyl oxygen atoms of a synthetic ester molecule. The phenomena observed during sample preparation also confirm this assumption. The maximal content molar ratios of LiTFSI in DEHA−LiTFSI, DEHS−LiTFSI, TMPTH−LiTFSI, and PETO−LiTFSI systems to form a homogeneous liquid phase (IL) are about 1/1.5, 1/1.5, 1/2 and 1/2, respectively. For these systems, if the molar ratios are 1/2, 1/2, 1/3, and 1/3, obvious solid LiTFSI residue can be observed.

Solubility. It was found that the in situ forming [Li(synthetic ester)]TFSI has a great effect on the solubility of LiTFSI in synthetic esters. Table 1 shows the comparing solubility of LiTFSI and conventional ILs in various synthetic esters. LiTFSI was found to have extremely good solubility in all the used esters. The solubility in DEHA is >54 wt %, in DEHS is >50 wt %, in TMPTH is about 57 wt % and in PETO is >33 wt % (the concentrations more than these values were not tested). Even stored at below −20 °C for several days, no solid LiTFSI will precipitate from these mixtures because of the in situ forming [Li(synthetic ester)]TFSI. This is a great advantage as compared with conventional ILs, which have very low solubility in synthetic esters. For example, L-F102 and L-F104 have the same anions as [Li(synthetic ester)]TFSI, but their solubility (<1.5 wt %) in all the used esters are far lower than that of LiTFSI. The solubility will become even lower as the carbon chain length of the ester increases. Because of the extremely low solubility, conventional ILs are hardly used as lubricant additives in synthetic esters.

Table 1. Comparison of the Solubility of LiTFSI and Conventional ILs in Various Synthetic Esters

synthetic esters	ILs	solubility (wt %)
DEHA	L-F102	1
DEHA	L-F104	1.5
DEHA	LiTFSI	>54
DEHS	L-F104	insoluble
DEHS	LiTFSI	>50
TMPTH	L-F104	1.5
TMPTH	LiTFSI	~57
PETO	L-F104	insoluble
PETO	LiTFSI	>33

Thermal Analysis. Figure 2a shows phase transition temperatures of DEHA/LiTFSI systems at various molar ratios. Only one endothermic peak related to the glass transition temperature (T_g) is observed in all the DSC traces of the DEHA-LiTFSI complex systems at molar ratios range from 8/1 to 1/1. The T_g increases with increasing LiTFSI content in the system. The T_g of pure DEHA occurs at −106.0 °C and those of the samples with LiTFSI at molar ratios 8/1 and 1/1 occur at −102.6 and −78.1 °C, respectively. The same phenomenon was also observed in the complex systems of DEHS−LiTFSI and TMPTH-LiTFSI at different molar ratios. This means that these systems remain as single phases and no solid LiTFSI precipitates in the measurement temperature range. Only for the system of PETO/LiTFSI, two endothermic peaks other than the freezing point of PETO (at about −19.9 °C) are observed at −57.0 and 17.9 °C for the samples at molar ratio more than 1/1. The former is the solidus temperature (T_s), while the latter is related to the liquidus temperature (T_l). The peak related to the freezing point of PETO disappears when the content of LiTFSI increases to 1/1. When the content increases to 1/2, however, only one weak endothermic peak related to T_g is observed at −76.4 °C. This means that this system remains as a single phase in the measurement temperature range.

Thermal analysis (DSC) also verifies addition of LiTFSI significantly increases the decomposition temperature (T_d) of synthetic esters as shown in Figure 3 and Table 2, indicating the enhancement of the thermal oxidation stability of all the esters.[21] Figure 3 shows the thermogravimetry (TG) curves of pure synthetic esters and synthetic ester−LiTFSI complex systems at molar ratio 1/1. The curves of all the complex systems show two-step weight loss processes. With a view to

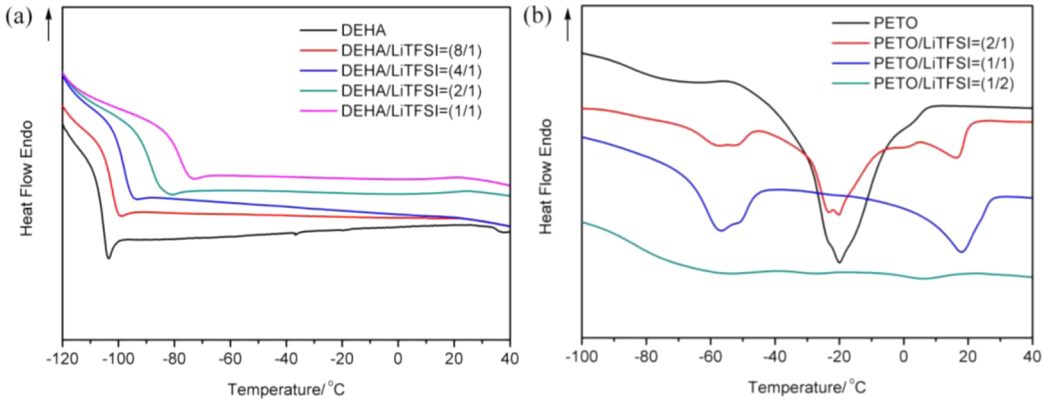

Figure 2. Typical DSC diagram of (a) pure DEHA and DEHA−LiTFSI and (b) pure PETO and PETO−LiTFSI complex systems at various molar ratios for determining the glass temperature (T_g), solidus temperature (T_s), liquidus temperature (T_l).

dx.doi.org/10.1021/am3018042 | ACS Appl. Mater. Interfaces 2012, 4, 6683−6689

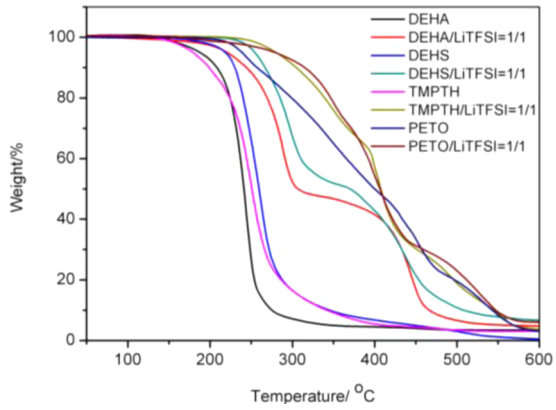

Figure 3. TG curves for pure synthetic ester and synthetic ester-LiTFSI complex systems at molar ratio 1/1.

Table 2. Performance Parameter for Pure Synthetic Ester and Synthetic Ester−LiTFSI Complex Systems at Molar Ratio 1/1

		TG temperature/°C per weight loss		
samples	T_d (°C)	10%	20%	50%
DEHA	217.1	219.1	229.1	244.1
DEHA/LiTFSI=1/1	248.4	254.4	274.4	354.4
DEHS	230.3	231.5	241.5	259.0
DEHS/LiTFSI=1/1	252.3	269.0	286.5	379.0
TMPTH	219.3	186.6	216.6	249.1
TMPTH/LiTFSI=1/1	229.8	265.5	290.5	390.5

the thermal properties of pure synthetic esters and LiTFSI, it is estimated that the initial loss is corresponding to the dissociation of coordination between Li^+ ions and esters and the pyrolysis of esters. The final step at temperatures higher than 400 °C is correlative with the thermal decomposition of LiTFSI. This thermal stability test further confirms the formation of ILs ([Li(synthetic esters)]TFSI) in the mixture of synthetic esters and LiTFSI.

Tribological Properties. Synthetic esters are commonly used lubricating oils, especially for combustion engines. In our experiment, one of the most used and commercially available adipate ester, Esterex adipate ester A51 (Esterex A51), was chosen as the base oil to test tribological properties of the in situ formed ILs. It is found that LiTFSI also has extremely good solubility in Esterex A51 (>40 wt %), whereas conventional ILs, such as L-B102, L-F102, L-F104, and L-P106, cannot dissolve in this oil. First, the viscosity, corrosion grade and thermal oxidation stability, important properties in lubrication, of Esterex A51 with different concentration of LiTFSI were tested and the results are shown in Table 3. It is seen that the viscosity of Esterex A51 increases slightly both at 40 °C and at 100 °C by the addition of LiTFSI. The increase in viscosity index indicates the enhancement of viscosity-temperature characteristics of the base oil. Also the thermal analysis verifies addition of LiTFSI significantly increases the decomposition temperature of Esterex A51, indicating the enhancement of the thermal oxidation stability of the base lubricating oil. For example, the temperature for 50% weight loss increases dramatically from 248.7 to 280.0 °C for 3 wt % LiTFSI added Esterex A51. Besides, the introducing of LiTFSI will not change the corrosion grade of the base oil according to the copper strip corrosion tests. All these tests verify the high feasibility of applying LiTFSI as lubricant additive.

In the following friction and wear tests, it was found that no significant improvement in tribological properties of Esterex A51 was observed at RT. But at high temperature as 100 or 150 °C, LiTFSI did improve the friction-reducing and antiwear properties of Esterex A51 dramatically. It is seen from Figure 4 that the addition of 1 wt % LiTFSI can greatly improve the friction-reducing and antiwear properties of Esterex A51. When the concentration increases to 3 wt %, the coefficient of friction (COF) reduces from above 0.16 to a very low level (~0.1) and the wear volume of the lower disc reduces by 27 times. Further increasing the content of LiTFSI above 4 wt % does not help with the friction-reducing and antiwear. The optimum concentration might be 1−3 wt %. From the photographs of inset in Figure 4, it is seen that the wear tracks can be visibly seen after friction with pure Esterex A51 and the oil color turns to light brown, indicating thermal oxidation reaction or the dissolution of wear debris, while the wear tracks are hardly found if lubricated with 3 wt % LiTFSI added Esterex A51 and the oil color has almost no change at all. In addition, the application scope of LiTFSI as lubricant additive was also investigated and found to be general to many synthetic esters. In all the used esters, including DEHA, DEHS, TMPTH and PETO, LiTFSI exhibits good friction-reducing and antiwear properties. The comparing average COF and wear volume are shown in Table 4.

Figure 5 displays the SEM micrographs of the worn surfaces of steel discs lubricated by pure Esterex A51 and 3 wt % LiTFSI added Esterex A51. It is clearly seen that the worn surface of the steel disc lubricated by pure Esterex A51 at 150 °C shows wider and deeper wear scar (5a, a′). Besides, obvious adhesive wear is observed and part of steel was torn off. The wear scars of steel disc lubricated by 3 wt % LiTFSI added Esterex A51 are comparatively narrow and shallow, and adhesive wear is greatly alleviated (5b, b′). These results are consistent with previously measured wear volume results and indicate undoubtedly the excellent antiwear property of LiTFSI as additive for Esterex A51.

Table 3. Physical Properties of Esterex A51 with Different Concentration of LiTFSI

	kinematic viscosity (mm^2/s)				TG temperature (°C) per weight loss		
lubricants	40 °C	100 °C	viscosity index	copper strip test/corrosion grade	10%	20%	50%
Esterex A51	26.79	128.67	5.22	1b	221.2	231.2	248.7
1% LiTFSI	27.97	129.61	5.36				
2% LiTFSI	29.65	129.64	5.59				
3% LiTFSI	30.93	130.15	5.72	1b	222.5	245.0	280.0
4% LiTFSI	33.10	130.21	6.04				
5% LiTFSI	34.38	130.76	6.21				

dx.doi.org/10.1021/am3018042 | ACS Appl. Mater. Interfaces 2012, 4, 6683−6689

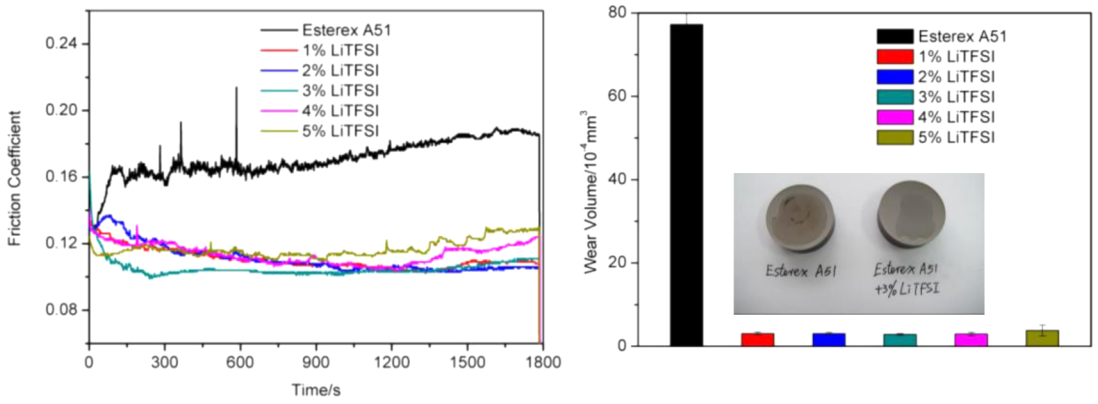

Figure 4. Evolution of friction coefficient/time and wear volume of the lower disks lubricated by different concentrations of LiTFSI in Esterex A51 at 150 °C (with load of 200 N and frequency of 25 Hz).

Table 4. Comparison of Average COF and Wear Volume Value of LiTFSI as Additives to Various Esters (With Load of 100 N and Frequency of 25 Hz at 150 °C)

base oils	average COF	standard deviation	wear volume/ 10^{-4} mm^3	standard deviation
DEHA	0.170	0.00436	26.69	1.4425
3% LiTFSI + DEHA	0.134	0.00645	4.76	0.3564
DEHS	0.157	0.01054	13.16	1.7466
3% LiTFSI + DEHS	0.120	0.00701	3.41	0.4676
TMPTH	0.167	0.00902	45.85	2.3900
3% LiTFSI + TMPTH	0.144	0.00729	2.72	0.6247
PETO	0.138	0.00924	18.55	1.7625
3% LiTFSI + PETO	0.125	0.01068	3.23	0.3591

X-ray photoelectron spectrometry (XPS) analysis of the worn surfaces was performed to verify the surface composition after friction. The XPS spectra are shown in Figure 6. It is seen that no obvious difference is observed on both the XPS spectra of Fe2p for worn steel surfaces lubricated by pure Esterex A51 and 3 wt % LiTFSI added Esterex A51. Also no characteristic peaks N1s and Li1s were detected on these worn steel surfaces. In the XPS spectra of O1s, peaks appear 530.2 and 531.8 eV for worn steel surface lubricated by Esterex A51, which may be ascribed to FeO, Fe_2O_3, Fe_3O_4, FeOOH, or Fe(OH)O.[22] The peak at 530.2 eV is higher than the peak at 531.8 eV. On the contrary, in the XPS spectra of O1s for worn steel surface lubricated by 3 wt % LiTFSI added Esterex A51, peaks appear 530.2 and 532.1 eV and the peak at 530.2 eV is lower than the peak at 532.1 eV. This indicates the generation of more abundant $FeSO_4$ or $Fe_2(SO_4)_3$ other than FeO, Fe_2O_3, Fe_3O_4, FeOOH or Fe(OH)O on the worn steel surface lubricated by LiTFSI. In the XPS spectra of F1s and S2p, no characteristic peaks were detected on the worn steel surface lubricated by pure Esterex A51. But in the XPS spectra of F1s, an obvious peak appears at 685.4 eV for worn steel surface lubricated by 3 wt % LiTFSI added Esterex A51. This value indicates the presence of abundant F^-, possibly because of the formation of FeF_2 or FeF_3. Similarly, in the XPS spectra of S2p, one peak appears at around 169.3 eV, which may be ascribed to $FeSO_4$,

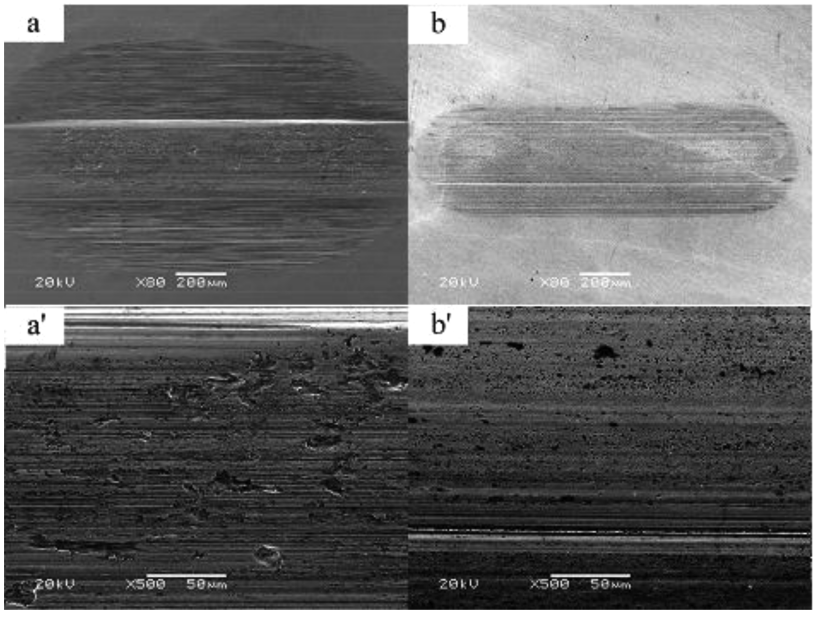

Figure 5. SEM micrographs of the worn surfaces lubricated by (a, a′) Esterex A51 and (b, b′) 3 wt % LiTFSI added Esterex A51.

dx.doi.org/10.1021/am3018042 | ACS Appl. Mater. Interfaces 2012, 4, 6683−6689

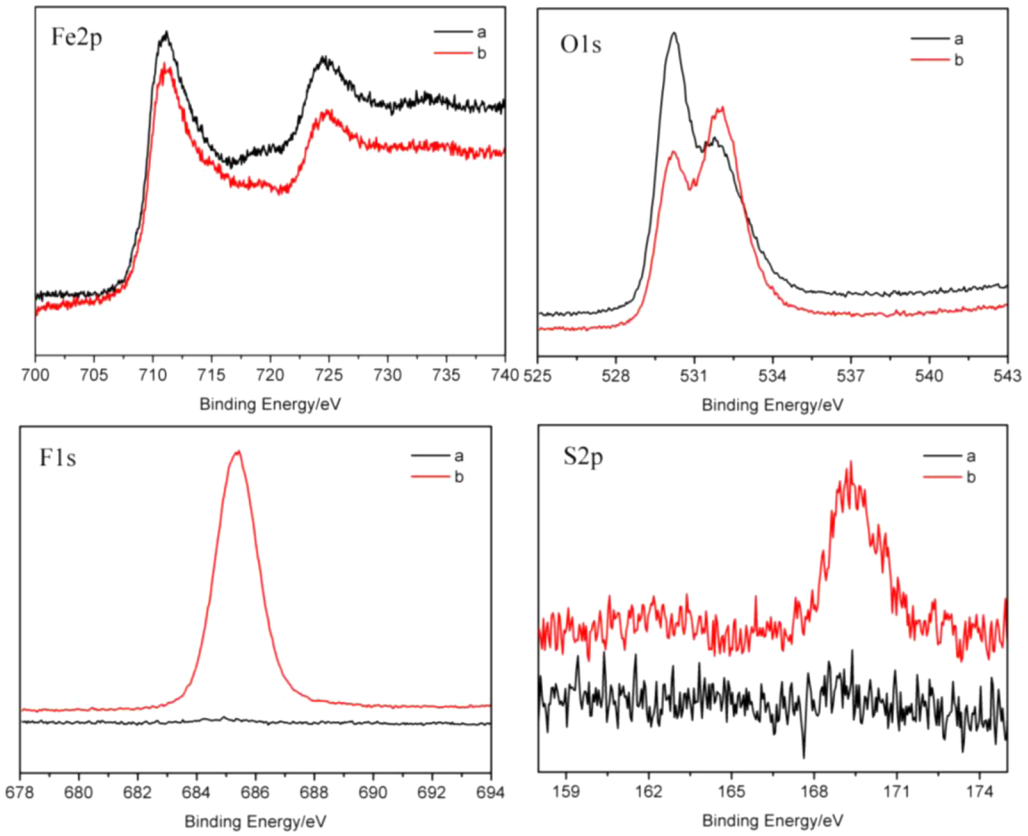

Figure 6. XPS spectra of the worn surfaces lubricated by different lubricants: (a) Esterex A51 and (b) 3 wt % LiTFSI added Esterex A51.

$Fe_2(SO_4)_3$, or organic sulfides (b). Thus, with the existing conditions, it is difficult to determine the exact tribological protective film species on the worn steel surfaces. But on the basis of the above data, it can be speculated minimally here that under a collective impact of high pressure, exoelectron emission, and frictional heating, complicated tribochemical reactions occur on the surfaces lubricated by LiTFSI. Thus some of the newly formed compounds, such as $FeSO_4$ or $Fe_2(SO_4)_3$, FeF_2, or FeF_3, coming from the reaction of additive with fresh metal were observed and acted as the protective film to prevent cold-welding of fresh metal and to alleviate wear. So in these cases, the excellent tribological properties are attributed to the polarity induced physical adsorption films of in situ formed ILs on the surfaces and further tribochemical reaction films of $TFSI^-$ with the sliding metallic surfaces.

From the mechanistic point of view, the good lubricating behavior of ILs is attributed to the polarity of their molecules and so their ability to form ordered adsorbed layers, resulting in the formation of physical adsorption protective films and further tribochemical reaction protective films on the sliding metallic surfaces.[23] Figure 7 shows the contact resistance during friction of sliding pairs. It is seen that the contact resistance drops to zero when lubricated with Esterex A51, indicating direct contact of asperities on both sliding pairs. However, obvious electrical resistance was measured when lubricated with 3 wt % LiTFSI added Esterex A51. This indicates obvious molecules absorption on sliding pairs to form effective protection film and so the separation and wear reduction of asperities by the absorbed molecules. This test result further confirms our proposed lubrication mechanism of the in situ formed ILs.

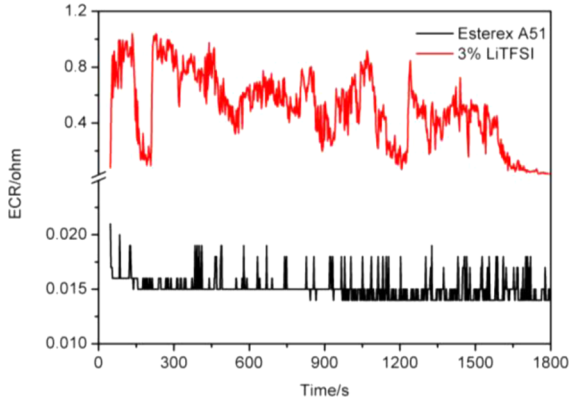

Figure 7. Contact resistance during lubrication with pure Esterex A51 and 3 wt % LiTFSI added Esterex A51 at 150 °C (with load of 200 N and frequency of 25 Hz).

In conclusion, LiTFSI can be used directly as lubricant additives for synthetic esters and found to have excellent friction-reducing and antiwear properties for the lubrication of steel/steel contacts. Its extremely good solubility in synthetic esters and excellent tribological properties are attributed to the in situ formation of ILs [Li(synthetic ester)]TFSI as the additives for base oils. The easy preparation, extremely good solubility and excellent tribological properties of [Li(synthetic ester)]TFSI show great advantages as compared with conventional ILs, which can hardly be used as lubricant additives in synthetic esters due to their low solubility. The present strategy expands the application scope of ILs in lubrication, especially the potential industrial application of IL additives in synthetic

esters that are very commonly used high performance lubricating oils for combustion engines.

AUTHOR INFORMATION

Corresponding Author

*E-mail: zhouf@licp.cas.cn (F.Z.); wmliu@licp.cas.cn (W.L.).

Notes

The authors declare no competing financial interest.

ACKNOWLEDGMENTS

The authors gratefully acknowledge the support of this work by NSFC (51105353, 21173243), Outstanding Young Scholarship (21125316), and 973 (2013CB632301).

REFERENCES

(1) Dupont, J.; de Souza, R. F.; Suarez, P. A. Z. *Chem. Rev.* **2002**, *102*, 3667−3692.
(2) Rogers, R. D.; Seddon, K. R. *Ionic Liquids as Green Solvents*; ACS Symposium Series 856; American Chemical Society: Washington, DC, 2002.
(3) Wasserscheid, P.; Welton, T. *Ionic Liquid in Synthesis*; Wiley-VCH Verlag: Weinheim, Germany, 2003.
(4) Han, X.; Armstrong, D. W. *Acc. Chem. Res.* **2007**, *40*, 1079−1086.
(5) MacFarlane, D. R.; Forsyth, M.; Howlett, P. C.; Pringle, J. M.; Sun, J.; Annat, G.; Neil, W.; Izgorodina, E. I. *Acc. Chem. Res.* **2007**, *40*, 1165−1173.
(6) Smiglak, M.; Metlen, A.; Rogers, R. *Acc. Chem. Res.* **2007**, *40*, 1182−1192.
(7) Minami, I. *Molecules* **2009**, *14*, 2286−2305.
(8) Bermúdez, M. -D.; Jiménez, A. -E.; Sanes, J.; Carrión, F.-J. *Molecules* **2009**, *14*, 2888−2908.
(9) Zhou, F.; Liang, Y.; Liu, W. *Chem. Soc. Rev.* **2009**, *38*, 2590−2599.
(10) Bonhôte, P.; Dias, A.-P.; Papageorgiou, N.; Kalyanasundaram, K.; Grätzel, M. *Inorg. Chem.* **1996**, *35*, 1168−1178.
(11) Hagiwara, R.; Ito, Y. *J. Fluor. Chem.* **2000**, *105*, 221−227.
(12) Fredlake, C. P.; Crosthwaite, J. M.; Hert, D. G.; Aki, S. N. V. K.; Brennecke, J. F. *J. Chem. Eng. Data* **2004**, *49*, 954−964.
(13) Greaves, T. L.; Drummond, C. J. *Chem. Rev.* **2008**, *108*, 206−237.
(14) Jiménez, A.-E.; Bermúdez, M.-D. *Wear* **2008**, *265*, 787−798.
(15) Fan, M. J.; Liang, Y. M.; Zhou, F.; Liu, W. M. *RSC Adv.* **2012**, *2*, 6824−6830.
(16) Watanabe, M.; Rikukawa, M.; Sanui, K.; Ogata, N.; Kato, H.; Kobayashi, T.; Ohtakilb, Z. *Macromolecules* **1984**, *17*, 2902−2908.
(17) Watanabe, M.; Togo, M.; Sanui, K.; Ogata, N.; Kobayashi, T.; Ohtakilb, Z. *Macromolecules* **1984**, *17*, 2908−2912.
(18) Rabek, J. F.; Lucki, J.; Qu, B. J.; Shis, W. F. *Macromolecules* **1991**, *24*, 836−843.
(19) Bonhôte, P.; Dias, A. P.; Papageorgiou, N.; Kalyanasundaram, K.; Grätzel, M. *Inorg. Chem.* **1996**, *35*, 1168−1178.
(20) Chen, R.; Wu, F.; Li, L.; Xu, B.; Qiu, X.; Chen, S. *J. Phys. Chem. C* **2007**, *111*, 5184−5194.
(21) Yoshida, K.; Nakamura, M.; Kazue, Y.; Tachikawa, N.; Tsuzuki, S.; Seki, S.; Dokko, K.; Watanabe, M. *J. Am. Chem. Soc.* **2011**, *133*, 13121−13129.
(22) National Institute of Standards and Technology. NIST X-ray Photoelectron Spectroscopy Database, version 4.1, 2012. http://srdata.nist.gov/xps/.
(23) Jiménez, A. E.; Bermúdez, M. D. *Tribol. Lett.* **2007**, *26*, 53−60.